SSD-TR-92-17

AEROSPACE REPORT NO.
TR-0091(6935-08)-1

Acoustic Measurement of the Mechanical Properties of Thin Material Specimens

Prepared by

E. C. JOHNSON, J. D. POLLCHIK, and J. N. SCHURR
Mechanics and Materials Technology Center
Technology Operations
The Aerospace Corporation

15 May 1992

Prepared for

SPACE SYSTEMS DIVISION
AIR FORCE SYSTEMS COMMAND
Los Angeles Air Force Base
P. O. Box 92960
Los Angeles, CA 90009-2960

Engineering and Technology Group

THE AEROSPACE CORPORATION
El Segundo, California

This report was submitted by The Aerospace Corporation, El Segundo, CA 90245-4691, under Contract No. F04701-88-C-0089 with the Space Systems Division. P. O. Box 92960, Los Angeles, CA 90009-2960. It was reviewed and approved for The Aerospace Corporation by R. W. Fillers, Principal Director, Mechanics and Materials Technology Center. Paul M. Propp was the project officer for the Mission-Oriented Investigation and Experimentation (MOIE) program.

This report has been reviewed by the Public Affairs Office (PAS) and is releasable to the National Technical Information Service (NTIS). At NTIS, it will be available to the general public, including foreign nationals.

This technical report has been reviewed and is approved for publication. Publication of this report does not constitute Air Force approval of the report's findings or conclusions. It is published only for the exchange and stimulation of ideas.

MARTIN K. WILLIAMS, Capt, USAF
Mgr, Space Systems Integration
DCS for Program Management

PAUL M. PROPP
Wright Laboratory West Coast Office
Materials Directorate

UNCLASSIFIED
SECURITY CLASSIFICATION OF THIS PAGE

REPORT DOCUMENTATION PAGE

1a. REPORT SECURITY CLASSIFICATION Unclassified	1b. RESTRICTIVE MARKINGS
2a. SECURITY CLASSIFICATION AUTHORITY	3. DISTRIBUTION/AVAILABILITY OF REPORT Approved for public release; distribution unlimited
2b. DECLASSIFICATION/DOWNGRADING SCHEDULE	
4. PERFORMING ORGANIZATION REPORT NUMBER(S) TR-0091(6935-08)-1	5. MONITORING ORGANIZATION REPORT NUMBER(S) SSD-TR-92-17
6a. NAME OF PERFORMING ORGANIZATION The Aerospace Corporation Technology Operations 6b. OFFICE SYMBOL *(If applicable)*	7a. NAME OF MONITORING ORGANIZATION Space Systems Division
6c. ADDRESS *(City, State, and ZIP Code)* El Segundo, CA 90245-4691	7b. ADDRESS *(City, State, and ZIP Code)* Los Angeles Air Force Base Los Angeles, CA 90009-2960
8a. NAME OF FUNDING/SPONSORING ORGANIZATION 8b. OFFICE SYMBOL *(If applicable)*	9. PROCUREMENT INSTRUMENT IDENTIFICATION NUMBER F04701-88-C-0089
8c. ADDRESS *(City, State, and ZIP Code)*	10. SOURCE OF FUNDING NUMBERS PROGRAM ELEMENT NO. / PROJECT NO. / TASK NO. / WORK UNIT ACCESSION NO.

11. TITLE *(Include Security Classification)*
Acoustic Measurement of the Mechanical Properties of Thin Material Specimens

12. PERSONAL AUTHOR(S)
Johnson, E. C.; Pollchik, J. D.; and Schurr, J. N.

13a. TYPE OF REPORT	13b. TIME COVERED FROM ____ TO ____	14. DATE OF REPORT *(Year, Month, Day)*	15. PAGE COUNT
		15 May 1992	21

16. SUPPLEMENTARY NOTATION

17. COSATI CODES			18. SUBJECT TERMS *(Continue on reverse if necessary and identify by block number)*
FIELD	GROUP	SUB-GROUP	Acoustic Velocity, Poisson's Ratio, Adhesives, Thin Materials, Modulus, Ultrasound

19. ABSTRACT *(Continue on reverse if necessary and identify by block number)*

An acoustic technique is presented which permits accurate measurement of the dynamic Poisson's ratio, and the Young's, shear, and bulk moduli for a specimen which exists as a thin (<10 mil) layer. This technique should prove especially useful in situations where a bulk specimen is either not readily available or would not properly reflect the properties of the material when configured as a thin layer. The report includes a detailed discussion of the theory underlying the technique. As a test, three materials which could be easily formed into both a thin specimen and a thick specimen were selected. The technique was then used to determine the Poisson's ratio and acoustic velocities of the material constituting each thin specimen. These values were then contrasted to those of the bulk specimens obtained in a more conventional manner. The technique, as presented, could be extended for a number of applications, including the cure monitoring of adhesives.

20. DISTRIBUTION/AVAILABILITY OF ABSTRACT	21. ABSTRACT SECURITY CLASSIFICATION
[X] UNCLASSIFIED/UNLIMITED [ ] SAME AS RPT. [ ] DTIC USERS	Unclassified

22a. NAME OF RESPONSIBLE INDIVIDUAL	22b. TELEPHONE *(Include Area Code)*	22c. OFFICE SYMBOL

DD FORM 1473, 84 MAR — 83 APR edition may be used until exhausted. All other editions are obsolete.

SECURITY CLASSIFICATION OF THIS PAGE
UNCLASSIFIED

CONTENTS

FIGURES

TABLE

I. INTRODUCTION

The Poisson's ratio for a material can be determined from the ratio of the acoustic shear velocity to the longitudinal velocity. These velocities can often be easily measured using conventional ultrasonic time-of-flight techniques. Over the years, however, difficulties associated with making velocity measurements on thin attenuative specimens have forced ultrasonic researchers to become more innovative. For example, in an early effort to measure the velocity of both transverse and longitudinal waves in a buna-N vulcanizate as a function of temperature, Nolle and Sieck (Ref. 1) employed a method involving the use of solid transmission media to conduct pulses into a thin, flat specimen. The error associated with the acoustic measurement, however, was estimated in the report to be as high as 5% and 10% for the longitudinal and shear wave data, respectively. Cunningham and Ivey (Ref. 2) improved upon the aforementioned technique by incorporating a double acoustic path comprised of two separate specimens. Again, however, a number of experimental difficulties (*e. g.*, producing uniform sample bond lines) contributed to significant measurement error. More recently, Kinra and Dayal (Ref. 3) report combining standard fast Fourier transform (FFT) methods with conventional ultrasonics to measure the longitudinal phase velocity in specimens of submillimeter thicknesses. Their report includes a brief summary and comparison of their technique to techniques recently developed by others, including the resonance method of Chang *et al.* (Ref. 4) and the phase insensitive tone-burst spectroscopic method of Heyman (Ref. 5).

This report presents a simple ultrasonic resonance technique which permits measurement of the Poisson's ratio of thin adhesive material specimens. The acoustic shear and longitudinal velocity are also determined. This technique is characterized by a number of advantages. For example, the Poisson's ratio measurement accuracy is limited only by that of the resonant frequency; the Poisson's ratio is independent of the thickness of the specimen. Also, the same specimen and transducer pair are used to determine both the shear and longitudinal response. In addition, a fluid medium is employed to couple sound into the specimen, thereby eliminating many of the problems associated with the bonding of transducers.

II. THEORY

The treatment which follows will be directed toward making Poisson's ratio measurements on thin (several mils thick) material specimens. The Poisson's ratio for a material can be determined through measurement of its acoustic velocities using the relation:

$$\sigma = \frac{c_l^2 - 2c_s^2}{2c_l^2 - 2c_s^2}, \tag{1}$$

where σ is the Poisson's ratio, and c_l and c_s are the longitudinal and shear acoustic velocities, respectively.

Consider first the semi-infinite medium (labeled Medium 1), with acoustic impedance Z_1, as depicted in Figure 1. If a thin layer of a second medium, Medium 2, with acoustic impedance Z_2, is placed in contact with the left side of Medium 1, the input impedance of the composite system (Medium 1 + Medium 2) is given by the complex relation:

$$Z_{21} = \frac{Z_2 Z_1 \cos(x_2\beta_2) + j\, Z_2^2 \sin(x_2\beta_2)}{Z_2 \cos(x_2\beta_2) + j\, Z_1 \sin(x_2\beta_2)}, \tag{2}$$

where j is the imaginary index and for Medium 2, x_2 is the thickness, $\beta_2 = 2\pi/\lambda_2$ is the propagation constant, and λ_2 is the acoustic wavelength (Ref. 6). Note that in the derivation of Eq. (2), a steady state condition (continuous plane wave stimulation of the system of frequency, f) was assumed. Wavelength is related to frequency according to the relation, $c = \lambda_2 f$, where c is the acoustic velocity (either shear or longitudinal) in Medium 2.

Next, consider what happens when a third (semi-infinite) medium, Medium 3, is placed in contact with the left side of Medium 2, as is also depicted in Figure 1. If this medium has the same acoustic impedance as that of Medium 1, then the stress wave reflection coefficient R is given by the relation:

$$R = \frac{Z_{21} - Z_1}{Z_{21} + Z_1} = \frac{Z_2 Z_1 \cos(x_2\beta_2) + j\, Z_2^2 \sin(x_2\beta_2) - Z_1\left(Z_2 \cos(x_2\beta_2) + j\, Z_1 \sin(x_2\beta_2)\right)}{Z_2 Z_1 \cos(x_2\beta_2) + j\, Z_2^2 \sin(x_2\beta_2) + Z_1\left(Z_2 \cos(x_2\beta_2) + j\, Z_1 \sin(x_2\beta_2)\right)}. \tag{3}$$

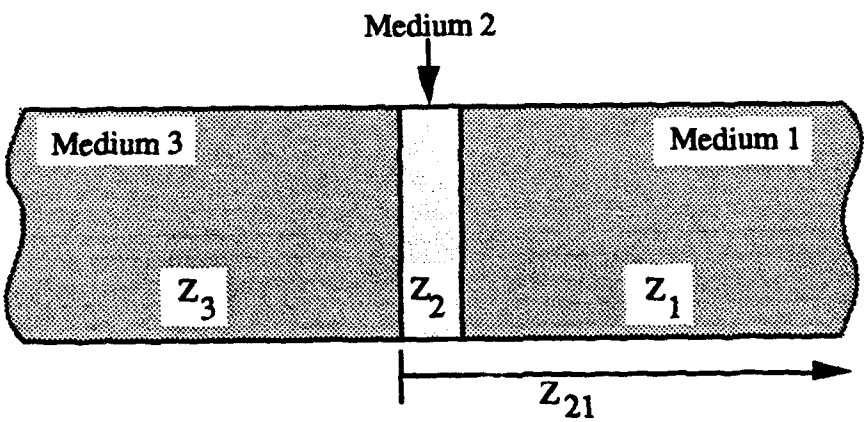

Figure 1. A thin medium of acoustic impedance Z_2, sandwiched between two semi-infinite media. Medium 3 sees the composite system formed by Medium 1 and Medium 2 as having an input acoustic impedance of Z_{21}.

The coefficient of acoustic power transfer P_T across Medium 2 can now be calculated:

$$P_T = 1 - |R|^2 = \frac{4 Z_2^2 Z_1^2}{\left(Z_1^2 + Z_2^2\right)^2 \sin^2\left(\frac{2\pi x_2 f}{c}\right) + 4 Z_2^2 Z_1^2 \cos^2\left(\frac{2\pi x_2 f}{c}\right)}, \tag{4}$$

where the substitution $\beta_2 = 2\pi c/f$ has been applied.

In Figure 2, P_T is plotted as a function of frequency for the case where Media 1 and 3 are aluminum (Z_1 = 17 rayls) and Medium 2 is water (Z_2 = 1.48 rayls). It can be seen that the condition of maximum power transmission occurs when $f = f_R = nc/2x_2$, where n is an integer. This behavior can be expected whenever Z_2 is higher than both Z_1 and Z_3 or lower than both Z_1 and Z_3 (as in this case). If Z_2 falls midrange between Z_1 and Z_3, maximum power transmission occurs when $f = f_R = (n+1)c/4x_2$. Note that Medium 2 was assumed to be lossless in the derivation of Eq. (4). Taking attenuation into account, one would expect the amplitude of the local maxima to decrease with increasing n. The expression for Poisson's ratio [Eq. (1)] can now be rewritten as

$$\sigma = \frac{f_{Rl}^2 - 2f_{Rs}^2}{2f_{Rl}^2 - 2f_{Rs}^2}, \tag{5}$$

where $f_{Rs} \propto c_s/2x_2$ and $f_{Rl} \propto c_l/2x_2$ are determined from the condition of maximum power transmission for shear and longitudinal acoustic waves, respectively.

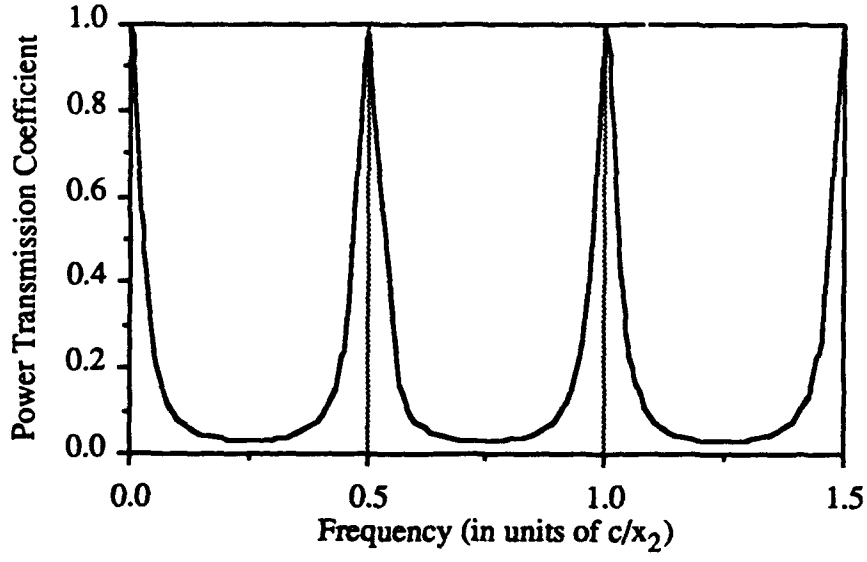

Figure 2. The coefficient of acoustic power transmission across Medium 2 as a function of frequency [Eq. (4)] for the three-layer system depicted in Figure 1, where $Z_1 = Z_3 = 17$ rayls (Al) and $Z_2 = 1.48$ rayls (H_2O).

III. TECHNIQUE

The experimental apparatus is depicted in Figure 3. Two aluminum blocks were cut from square rod stock, each having a 74° and 90° face with respect to one side of the block. A milled finish was determined to be adequate on the 74° faces. The 90° faces were lapped to ensure that the surfaces were flat. A thin, uniform layer of the specimen being tested was sandwiched between the 90° faces. The spacing between these faces and, hence, the specimen thickness, was determined by two identical stainless steel wire spacers. To hold this Al/specimen/Al sandwich together, a small rubber O-ring was stretched over a set of threaded pegs located on each of two opposite sides of the sandwich as shown. The depth of thread for these pegs was less than 0.125 inch. The resultant Al/specimen/Al sandwich was set upon a fixture (not included in Figure 3 for clarity) and submerged in a water tank in order to be centered between a pair of 5 MHz plane wave, through-transmission ultrasonic transducers. The fixture was designed to permit rotation of the specimen with respect to the transducers. The apparatus is designed to approximate the conditions leading to the derivation of Eq. (4). The Al blocks correspond to Media 1 and 3, the specimen to Medium 2.

To perform measurements, one transducer was stimulated to propagate a tone-burst (single frequency) longitudinal drive pulse (water will not support a shear wave). The fixture was aligned so that this pulse would strike the first 74° face of the Al/specimen/Al sandwich at a particular angle of incidence θ_i to its normal, giving rise to both a longitudinal and a shear wave pulse within the aluminum, with angles of emergence θ_l and θ_S, respectively. The emergence angles for a particular θ_i can be determined by the well-known Snell's law analog,

$$\frac{\sin\theta_i}{\sin\theta_s} = \frac{V_w}{V_s} \quad \text{and} \quad \frac{\sin\theta_i}{\sin\theta_l} = \frac{V_w}{V_l} . \tag{6}$$

where V_w is the acoustic velocity in water, and V_s and V_l are the acoustic velocities for shear and longitudinal waves in aluminum, respectively.

In the first phase of the experiment, θ_i was set at ~ 3.7°, so that the longitudinal pulse transmitted through the first 74° face would strike the Al/specimen interface at normal incidence. This pulse would then travel through the remainder of the Al/specimen/Al sandwich to produce a

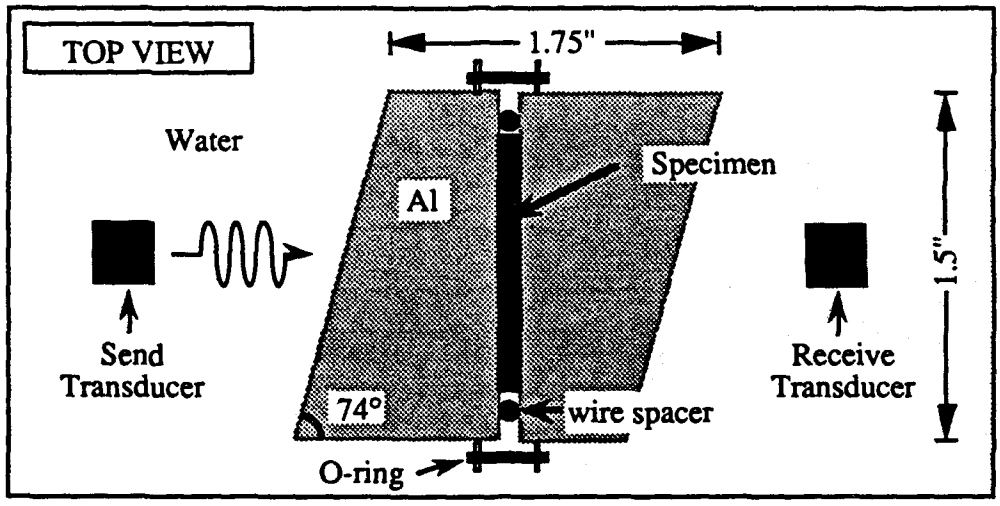

Figure 3. The experimental apparatus as described in the text. As indicated, this is a top view. The Al/specimen/Al sandwich extends 1.5 inches into the page. The transducers and O-ring are bisected by a plane parallel to that of the page and 0.75 inch into the page.

signal at the receive transducer, as depicted in Figure 4a. This signal will be referred to as the longitudinal response. Because the longitudinal velocity in Al exceeds that of the shear, the longitudinal response was the first signal detected after each drive pulse. This first signal was followed by others due to the shear wave transmitted through the first 74° face and various internal reflections within the sandwich. The duration of the drive pulse was chosen to be ~1.5 μs, which was short enough to permit temporal separation of the various signals, yet long enough to allow reverberations within the thin specimen layer to approximate a steady state (*i. e.*, these reverberations did not significantly affect the lengths of the pulses). The amplitude of the longitudinal response was measured as a function of frequency (between 2 and 8 MHz). To isolate the effect of the specimen, the Al/specimen/Al sandwich was then replaced with a solid Al block of the same dimensions, and the measurement was repeated. This second set of data was divided into the first set. The resultant data set was then normalized and plotted. Peaks in the the amplitude vs. frequency plot--which, in accordance with Eq. (4), occur when $f = f_{Rl} = nc_l/2x_2$--were then used to determine c_l, the longitudinal acoustic velocity of the specimen.

In the second phase of the experiment, θ_i was set to ~ 7.5°, so that the direction of the transmitted shear wave was normal to the Al/specimen interface, as depicted in Figure 4b. The first signal resulting from this normal shear pulse will be referred to as the shear response. Following each drive pulse, the shear response was preceded by not only the longitudinal response, but also by other signals resulting from internal reflections involving the faster longitudinal pulse. To positively identify the shear response, one could increase θ_i beyond the critical angle for longitudinal wave production in the aluminum, so that the shear response would be the first remaining signal. One could then track this signal while decreasing θ_i to the appropriate value. The frequency dependence of the shear response amplitude was then measured, normalized, and plotted in the same manner as that of the longitudinal response amplitude. Peaks in this plot, occurring when $f = f_{Rs} = nc_s/2x_2$, were then used to determine the shear acoustic velocity of the specimen, c_s.

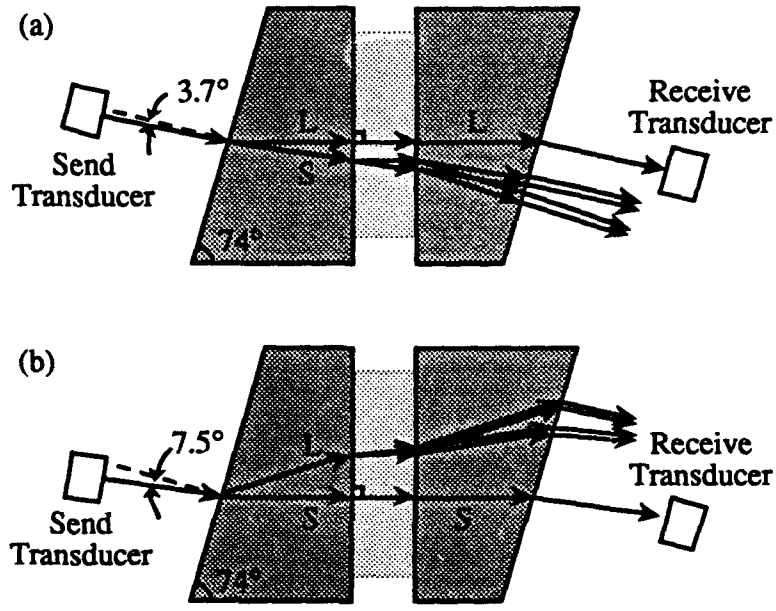

Figure 4. Ray diagrams for the apparatus depicted in Figure 3. The specimen thickness has been enlarged for clarity. In (a), to measure c_l, a pulse is emitted with a wavevector at 3.7° to the normal for the 74° face. Mode conversion at the surface results in a longitudinal wave pulse (denoted by L) which traverses the Al/specimen/Al sandwich in a direction normal to the Al/specimen interface. This is the first signal to reach the receive transducer. A slower shear wave pulse (denoted by S) is also generated. As indicated, this pulse gives rise to a number of additional pulses (both shear and longitudinal). Care must be taken to identify the signal of interest. To generate a shear wave pulse normal to the Al/specimen interface, the configuration displayed in (b) was used.

IV. RESULTS

Before both c_s and c_l were measured in a material, a simpler system having no shear response was tested. An $Al/H_2O/Al$ sandwich with wire spacers that had a diameter of $x_2 = 1.016 \times 10^{-4}$ m (4 mils) was prepared. It should be emphasized that in this case (and all cases that follow), the 90° faces on the Al blocks were lapped flat with 600 grit garnet. Earlier tests, using blocks which had not been lapped, yielded results which were not satisfactory. In Figure 5, the frequency response of the $Al/H_2O/Al$ sandwich and a solid Al standard are plotted as boxes and circles, respectively. The second plot was divided into the first plot and normalized to produce the solid curve. The importance of this correction (for the transducer response and attenuation in the Al) is obvious. The peak in the solid curve, at $f_R = 7.3$ MHz, was used to calculate $c_l \approx 2f_{Rl}x_2 = 1483$ m/s for water, in excellent agreement with the literature value.

Three materials--Black Wax (BW), Five Minute Epoxy (FME), and Crystalbond (CB) adhesive--were selected for measurement of both c_s and c_l. These materials were easily obtained and could be easily formed into both a thin specimen, as needed for this experiment, and a thick specimen, for comparative purposes. The longitudinal response and shear response data for the thin Black Wax specimen are plotted in Figure 6. The raw data were corrected, as outlined above, to produce these curves. The wire spacers used for the Al/BW/Al sandwich had a diameter of 2.39×10^{-4} m (9.4 mils). The longitudinal response exhibits a peak at 4.8 MHz, corresponding to a longitudinal velocity of 2290 m/s. The shear response curve exhibits four equally spaced peaks, corresponding to n = 1, 2, 3, and 4 in the relation; $f_{Rs} = nc_s/2x_2$. As expected, the amplitude of these peaks decreases with increasing n, due to attenuation within the black wax. Note that the data become less reliable as one pushes the limits on the operating range of the transducer (see the circle plot of Figure 5). The positions of the shear peaks correspond to a shear velocity of $c_s = 1120$ m/s. As mentioned earlier, a thick specimen of black wax was also prepared with the approximate dimensions of 2.5 x 2.5 x 0.66 cm. The longitudinal and shear velocities of this specimen were measured using a standard through-transmission, ultrasonic technique. Table 1 compares the values thus obtained to those for the thin specimen, along with similar results which were obtained for

Crystalbond adhesive and Five Minute Epoxy. The entrees for Poisson's ratio were calculated using Eq. (5).

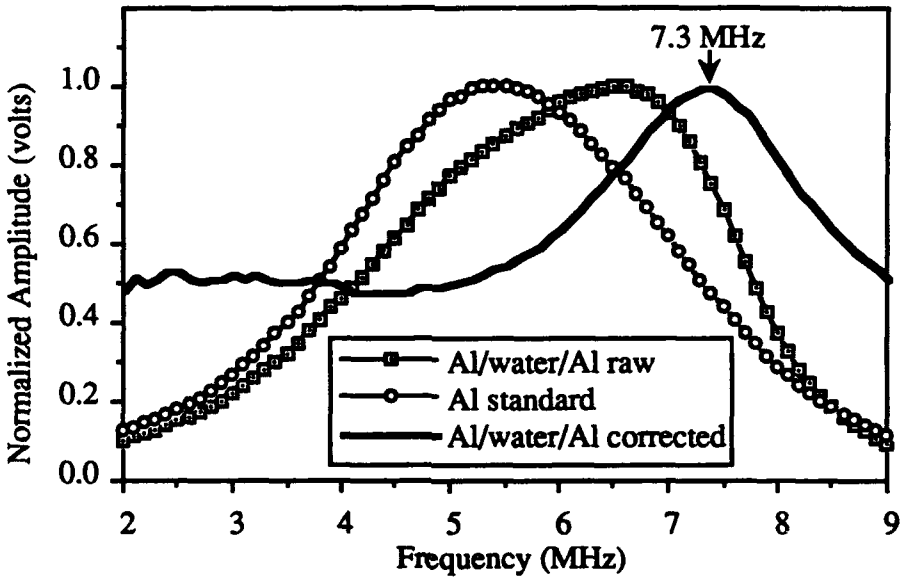

Figure 5. Sample data for an Al/H_2O/Al sandwich. The wire spacers for this sandwich had a diameter of $x_2 = 1.016 \times 10^{-4}$ m (4 mils). The circles result from a measurement of the frequency response of a solid aluminum standard of the same dimensions as the sandwich. Dividing the data from the standard into the raw Al/H_2O/Al data (boxes) corrects for both the attenuation due to the aluminum and the transducer response, thereby isolating the effect of the H_2O layer. The resulting solid curve exhibits a peak at 7.3 MHz, which can be used to calculate $c_l = 2f_{Rl}x_2 = 1483$ m/s for water, in close agreement with the book value, 1483 m/s (Ref. 6).

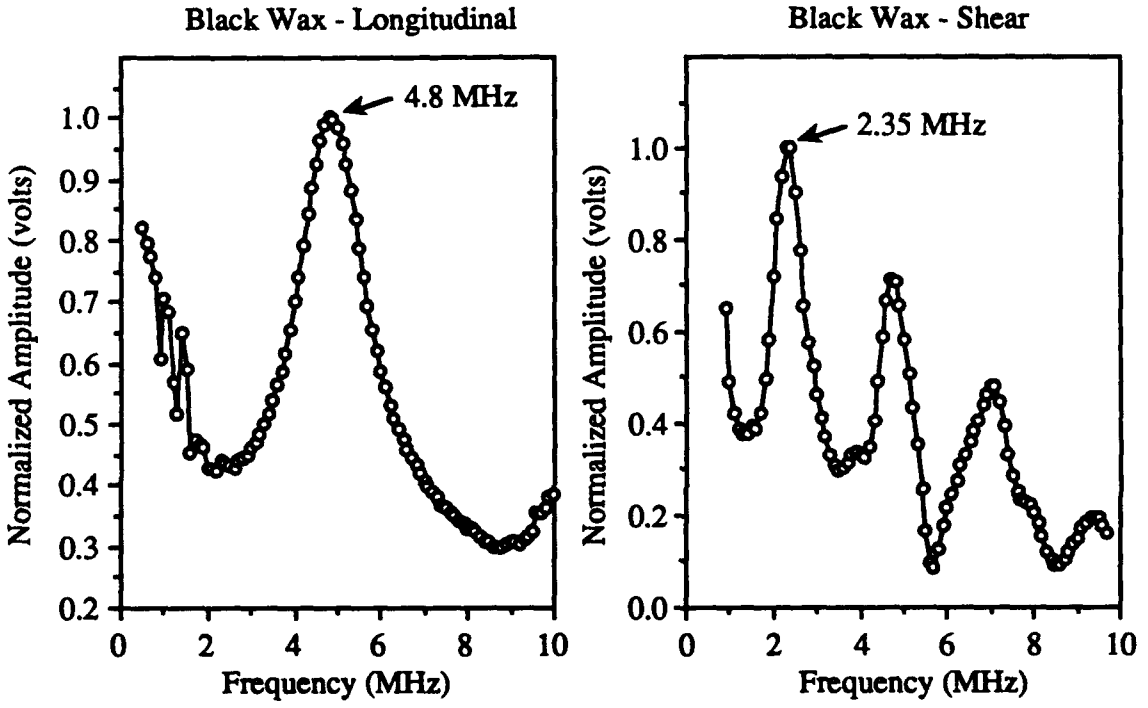

Figure 6. Data for black mounting wax. The wire spacer had a diameter of 2.39 x 10^{-4} m (9.4 mils).

Table 1. Comparison of Velocities Measured for Thin and Thick Specimens

	c_l (10^5 cm/s)		c_s (10^5 cm/s)		σ	
Sample	Thin	Thick	Thin	Thick	Thin	Thick
BW[a]	2.29	2.23	1.12	1.11	0.364	0.355
CB[b]	2.33	2.3	1.12	1.15	0.350	0.333
FME[c]	2.7	2.7	1.25	1.28	0.343	0.335

[a]Black wax.
[b]Crystalbond adhesive.
[c]Five Minute Epoxy.

V. DISCUSSION

It can be observed that for the three materials tested, the resonance technique for thin specimens described in this report leads to values for c_l, c_s, and σ which compare well with values determined using thicker specimens and a conventional through-transmission ultrasonic method (Table 1). The two techniques yield values that differ by only a few percent. This difference falls within the uncertainty ascribed to the conventional measurement. When used to measure the acoustic velocity of water, the resonance technique yielded a value essentially equivalent to that reported in the literature. Sources of error for the resonance technique include error in determination of the resonant frequency, wire thickness, and sample alignment, or nonuniformities in the specimen thickness, which lead to a broadening of the resonance. The resonant frequency can be determined more accurately by sampling with a finer frequency increment. Problems with specimen alignment can be mitigated through a well-designed apparatus and careful experimentation. The wire thickness is important for determination of the velocities but drops out of the equation for the Poisson's ratio.

The resonance technique presented should prove particularly useful for measurement of the mechanical properties of materials which exist (perhaps only) as thin (subwavelength) layers, such as adhesives or highly attenuative materials. The use of a fluid couplant medium provides for uniform and repeatable coupling of the sound into the specimen. The capability for measuring both velocities on a single sample becomes especially useful when multi-component polymer systems are being tested, because of the variations within and between batches. In addition to the Poisson's ratio and acoustic velocities, if the density, ρ, of the specimen is known, the Young's, shear, and bulk moduli, E, μ, and K, can also be calculated via the familiar relations,

$$E = \frac{\rho c_l^2 (1 - 2\sigma)(1 + \sigma)}{1 - \sigma}, \quad \mu = \rho c_s^2 \quad \text{and} \quad K = \frac{E}{3(1 - 2\sigma)}. \tag{7}$$

It is implicit that the properties measured are dynamic. In many instances, however, the temperature of the specimen and/or the frequency of measurement can be arranged so that the measurement occurs well above or below the glass transition.

In addition to the aforementioned applications, a number of enhancements and/or extensions of the technique can be envisioned. Instead of using a tone-burst signal and

sweeping the frequency, one might instead use a broadband pulse and Fourier transform the received signal. One could then effectively get all the information from a single pulse. The technique could also be arranged to study or monitor the cure of adhesives.

REFERENCES

1. A. W. Nolle and P. W. Sieck, J. Appl. Phys, **23**, 888 (1952).
2. J. R. Cunningham and D. G. Ivey, J. Appl. Phys., **27**, 967 (1956).
3. V. K. Kinra and V. Dayal, Experimental Mechanics, **28**, 289 (1988).
4. F. H. Chang, J. C. Couchman and B. G. W. Yee, J. Comp. Mat., **8**, 356 (1974).
5. J. S. Heyman, J. Acoust. Soc. Amer., **64**, 243 (1968).
6. G. S. Kino, Acoustic Waves: Devices, Imaging and Analog Processing (Prentice-Hall, 1987), p.12.

TECHNOLOGY OPERATIONS

The Aerospace Corporation functions as an "architect-engineer" for national security programs, specializing in advanced military space systems. The Corporation's Technology Operations supports the effective and timely development and operation of national security systems through scientific research and the application of advanced technology. Vital to the success of the Corporation is the technical staff's wide-ranging expertise and its ability to stay abreast of new technological developments and program support issues associated with rapidly evolving space systems. Contributing capabilities are provided by these individual Technology Centers:

Electronics Technology Center: Microelectronics, solid-state device physics, VLSI reliability, compound semiconductors, radiation hardening, data storage technologies, infrared detector devices and testing; electro-optics, quantum electronics, solid-state lasers, optical propagation and communications; cw and pulsed chemical laser development, optical resonators, beam control, atmospheric propagation, and laser effects and countermeasures; atomic frequency standards, applied laser spectroscopy, laser chemistry, laser optoelectronics, phase conjugation and coherent imaging, solar cell physics, battery electrochemistry, battery testing and evaluation.

Mechanics and Materials Technology Center: Evaluation and characterization of new materials: metals, alloys, ceramics, polymers and their composites, and new forms of carbon; development and analysis of thin films and deposition techniques; nondestructive evaluation, component failure analysis and reliability; fracture mechanics and stress corrosion; development and evaluation of hardened components; analysis and evaluation of materials at cryogenic and elevated temperatures; launch vehicle and reentry fluid mechanics, heat transfer and flight dynamics; chemical and electric propulsion; spacecraft structural mechanics, spacecraft survivability and vulnerability assessment; contamination, thermal and structural control; high temperature thermomechanics, gas kinetics and radiation; lubrication and surface phenomena.

Space and Environment Technology Center: Magnetospheric, auroral and cosmic ray physics, wave-particle interactions, magnetospheric plasma waves; atmospheric and ionospheric physics, density and composition of the upper atmosphere, remote sensing using atmospheric radiation; solar physics, infrared astronomy, infrared signature analysis; effects of solar activity, magnetic storms and nuclear explosions on the earth's atmosphere, ionosphere and magnetosphere; effects of electromagnetic and particulate radiations on space systems; space instrumentation; propellant chemistry, chemical dynamics, environmental chemistry, trace detection; atmospheric chemical reactions, atmospheric optics, light scattering, state-specific chemical reactions and radiative signatures of missile plumes, and sensor out-of-field-of-view rejection.